Available online at www.sciencedirect.com
SCIENCE DIRECT®
Journal of Nuclear Materials 329–333 (2004) 416–419
journal of nuclear materials
www.elsevier.com/locate/jnucmat

Creep rupture properties of helium implanted V–4Cr–4Ti alloy NIFS-HEAT-2

Toshinori Chuto [a,*], Norikazu Yamamoto [a], Johsei Nagakawa [a,b], Yoshiharu Murase [a]

[a] National Institute for Materials Science, 1-2-1, Sengen, Ibaraki, Tsukuba 305-0047, Japan
[b] Interdisciplinary Graduate School of Engineering Sciences, Kyushu University, 6-1 Kasuga Koen, Kasuga, Fukuoka 816-8580, Japan

Abstract

The influence of transmutational helium on creep response of a V–4Cr–4Ti reference alloy called NIFS-HEAT-2 was examined. This is a candidate structural material for future fusion applications. Helium ions were injected into creep specimens at 700 °C to a concentration of about 100 appm utilizing homogenous α-particle irradiation at an accelerator. Post-implantation creep rupture tests were carried out at the same temperature in a vacuum environment. Creep lifetime had a tendency to be increased by helium implantation, reflecting a slight decrease in minimum creep rate. Creep data showed a power-law creep behavior, and there was good agreement in obtained stress exponents between helium implanted and unimplanted cases. Some morphological changes were detected on creep-ruptured surfaces, such as reduction of necking and initiation of intercrystalline separation.

1. Introduction

Vanadium-base alloys have been identified as attractive high-performance structural materials for first-wall and blanket components in fusion power systems [1]. Based on the results from previous investigations, a V–4Cr–4Ti alloy is considered to be a leading candidate at present. Recently, large heats of high-purity V–4Cr–4Ti alloy called NIFS-HEAT were produced in NIFS (National Institute for Fusion Science) [2]. Plates, sheets and wires fabricated from those heats were supplied to a number of research groups to be investigated under international collaboration programs.

One of the advantages of vanadium alloys for fusion applications is their high material performance at elevated temperatures. The upper temperature limit for vanadium alloys is assumed to be 700–750 °C, and is most probably determined by compatibility with the fusion environment, the effect of gaseous transmutants such as helium, and mechanical properties such as tensile properties and creep resistance [3]. Thermal creep properties of V–4Cr–4Ti alloy have been investigated by uniaxial tensile and biaxial pressurized tube specimens [4–6]. The data base on irradiation creep is still very limited but has been accumulated gradually. On the other hand, effects of transmutation-produced helium on material properties, especially on creep, are the most uncertain factors. A large amount of helium, such as will be generated in fusion environment often causes a deterioration of high-temperature mechanical properties, the so-called helium embrittlement. Such mechanical degradation by helium at elevated temperatures is known to arise more markedly in long-term experiments rather than short time examinations such as tensile tests [7,8]. Therefore long-time experiments are crucial for investigation of helium effects on material properties. In this study, in order to investigate the influence of helium on creep properties of a V–4Cr–4Ti reference alloy, NIFS-HEAT-2, creep rupture tests were carried out using uniaxial creep specimens containing helium. The neutronic production of helium in a fusion environment

* Corresponding author. Tel./fax: +81-29-859-2014.
E-mail address: chuto.toshinori@nims.go.jp (T. Chuto).

0022-3115/$ - see front matter © 2004 Elsevier B.V. All rights reserved.
doi:10.1016/j.jnucmat.2004.04.077

was simulated by homogeneous α-implantation using a cyclotron accelerator.

2. Experimental

The material used in this experiment was a newly-developed V–4Cr–4Ti reference alloy (NIFS-HEAT-2). It contains the following chemical elements in weight percentage: 4.02 Cr, 3.98 Ti, 0.0069 C, 0.0148 O, 0.0122 N. Plates of 1.9 mm in thickness were supplied by NIFS in the 93% cold-worked and process annealed (1000 °C for 7.2 ks) condition. The plates were cold-rolled to about 0.09 mm thick sheets. Creep test specimens were prepared by punching from the sheets and polishing the surfaces on emery paper to the final thickness that had been determined by the projected range of α-particles mentioned below. The dimension of the gauge section was 10 mm in length, 4 mm in width and 0.085 mm in thickness. All the test samples were annealed at 950 °C for 3.6 ks in a vacuum of about 1×10^{-5} Pa, wrapped with Ta and Zr foils to obtain a fully re-crystallized condition. The mean grain size was measured 15.1 μm.

Helium implantation was carried out in a vacuum of about 3×10^{-4} Pa using a 20 MeV α-beam from the NIMS (National Institute for Materials Science) compact cyclotron. A Zr foil of 20 μm in thickness was fixed in front of the specimen holder as an impurity absorber. The projected range of the energy-degraded beam through the Zr foil was computed to be 85.1 μm by the SRIM 96 code, which was enough to penetrate the specimen thickness noted above. The energy of α-particles was moderated with a rotating energy absorber consisting of Al foils with 16 different thicknesses in order to obtain a homogeneous helium deposition along the injected direction in the specimen. In addition, the beam was scanned in the other two directions so as to attain a uniform distribution all over the specimen gauge length and width. The specimens were irradiated at 700 °C to helium contents of about 100 appm with a dose rate of 1×10^{-3} appm He/s. The irradiation temperature was measured with two thermocouples spot welded on a dummy plate situated in the middle of the irradiated area. Temperature variation due to beam fluctuation was compensated by adopting an infrared lamp heater with rapid response, and suppressed to within 4 °C during the implantation.

Creep rupture tests were also performed at 700 °C in a vacuum of $<2\times10^{-5}$ Pa using electro-mechanically controlled machines. In this machine, the applied load is monitored with a load cell mounted in a vacuum chamber and a load deviation from the stated value is canceled by cross head motion based on feedback signals. The shifts of load and temperature from nominal values during creep tests were maintained less than ±1 MPa and ±1 °C, respectively. The creep elongation was measured to a high precision of few μm with two linear variable differential transformers that were both connected to a rotary encoder. In addition to the implanted specimens, creep tests in the same manner were carried out on helium free reference samples which were not irradiated but underwent the same thermal history as the corresponding implanted ones. After the tests, fracture surfaces of failed specimens were examined by scanning electron microscopy (SEM) in order to mainly characterize the fracture mode.

Experimental details and equipment have been described in an earlier publication [9].

3. Results and discussion

Fig. 1 shows typical creep strain-time readings of helium free and implanted samples, which were loaded with almost the same applied stress. For all tests, the creep rupture time of the helium bearing samples increased by a factor of 2–3 compared to that of the unimplanted ones. As shown in the figure, the minimum creep rate was decreased and the secondary creep portion of the curve became large by helium implantation. All the samples showed a small tertiary creep strain, which would be responsible for the smaller rupture elongation relative to the previous results of uniaxial creep tests on V–4Cr–4Ti alloys.

Dependence of the minimum creep rate on applied stress is presented in Fig. 2. The minimum creep rate had a tendency to be decreased slightly by the irradiation. It is considered that these changes in creep properties, that is, slight increase in the creep lifetime and decrease in the minimum creep rate, can be correlated with irradiation hardening presumably due to radiation-enhanced precipitation and formation of helium clusters in the matrix. However, microstructural observation of the

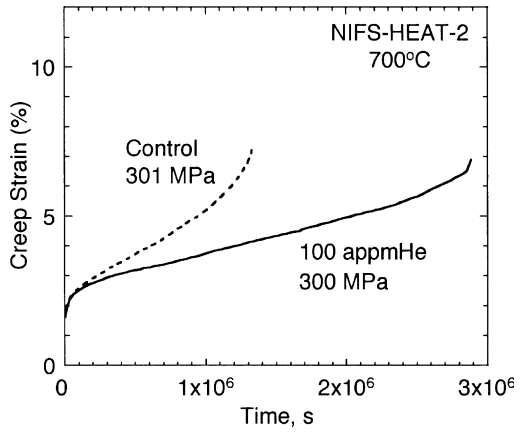

Fig. 1. Comparison of creep curves of a helium implanted specimen and an unimplanted control of V–4Cr–4Ti alloy NIFS-HEAT-2 tested at 700 °C.

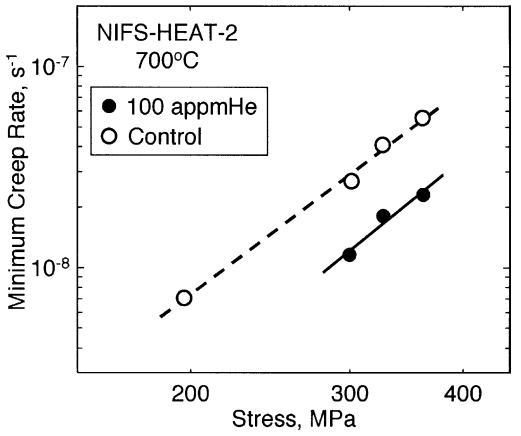

Fig. 2. Minimum creep rate as a function of applied stress at 700 °C for helium implanted specimens and corresponding controls of the V–4Cr–4Ti alloy NIFS-HEAT-2.

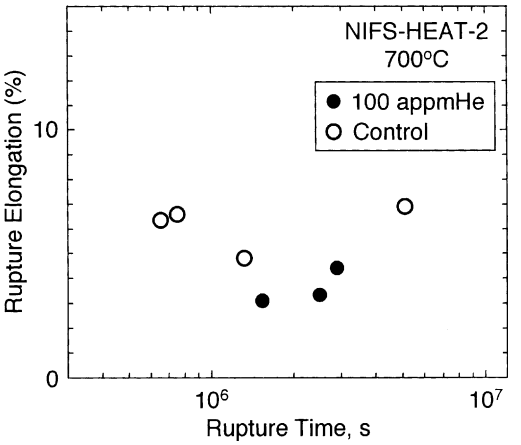

Fig. 3. Creep rupture elongation as a function of creep rupture time at 700 °C for helium implanted specimens and corresponding controls of the V–4Cr–4Ti alloy NIFS-HEAT-2.

specimens has not done yet. All the data in Fig. 2 were fitted to a creep power law for the minimum creep rate, $\dot{\varepsilon}_{MCR} \propto \sigma^n$, and the stress exponent (n) obtained was 3.7 for the implanted specimens and 3.4 for the unimplanted ones. The coefficient in both cases was again revealed to be nearly equal, and close to the previous results of uniaxial thermal creep tests using 1 mm thick specimens [6]. This result implies that the creep mechanism itself would not be changed by helium implantation.

The elongation at rupture is plotted in Fig. 3 as a function of creep rupture time. The scatter of the data points seems to be within normal experimental errors. However, because of the large scatter of data and limited number of data, it is difficult to identify any dependence of rupture elongation on rupture time. The average values of the elongation were $(3.6 \pm 1.4)\%$ and $(6.2 \pm 1.8)\%$ for helium implanted and unimplanted specimens, respectively. The rupture elongation decreased slightly after helium implantation.

Fig. 4 shows typical fracture surfaces of helium free reference and implanted samples tested at 300 MPa. Fig. 4(c) was taken from another part of the implanted sample (b) at higher magnification. All of the control samples failed in a perfectly transgranular ductile manner showing a mixture of the wedge type fracture and the dimple pattern (Fig. 4(a)). Thinning of the cross section in the fracture zone was significant and the regions of the dimple fracture were less than 10%. Most of the fracture surfaces of helium injected specimens also showed a ductile fracture mode (Fig. 4(b)), but the regions of dimple pattern increased and the reduction in area decreased compared with the controls. Fig. 5 compares the reduction in area between helium implanted specimens and unirradiated control samples as a function of applied stress. On average, the reduction in area was 50% and 95% for helium implanted and unimplanted cases, respectively. In addition to the reduction of necking, a part of the fracture surfaces were observed to contain intergranular decohesion induced by helium (Fig. 4(c)). The ratio of the intergranular fracture regions to the whole of the fracture zone ranged from 5% to 15%. It seems that degradation induced by helium and strengthening due to irradiation had simultaneously occurred in this irradiation condition. The stronger contribution of the latter may have resulted in no effectual degradation of creep properties, whereas detrimental effects of helium were recognized as the morphological changes on the ruptured surfaces. It is possible that drastic degradation of creep properties will arise at higher helium concentrations.

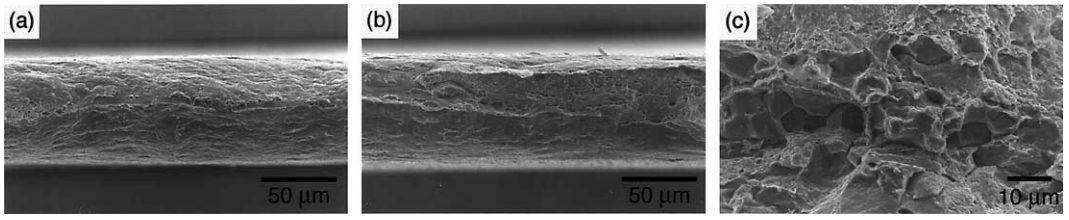

Fig. 4. Typical fracture surfaces of the V–4Cr–4Ti alloy NIFS-HEAT-2 creep tested at 700 °C, 300 MPa; (a) helium free reference ($t_r = 1.33 \times 10^6$ s), (b) and (c) helium implanted sample ($C_{He} = 100$ appm, $t_r = 2.88 \times 10^6$ s).

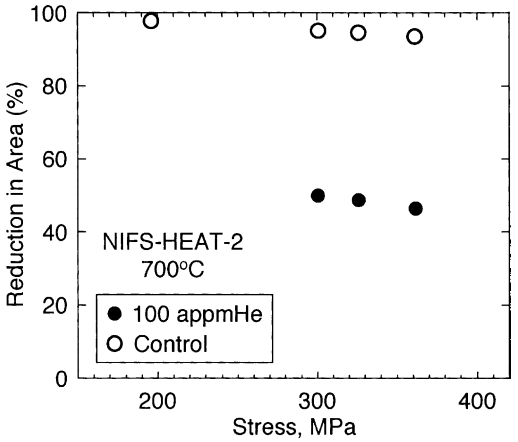

Fig. 5. Reduction in area as a function of applied stress at 700 °C for helium implanted specimens and corresponding controls of the V–4Cr–4Ti alloy NIFS-HEAT-2.

4. Summary

Creep rupture tests at 700 °C were performed on a low activation V–4Cr–4Ti reference alloy, NIFS-HEAT-2, after hot helium implantation ($T_{\text{impl.}} = 700$ °C, $C_{\text{He}} = 100$ appm).

(1) Creep rupture times of helium bearing samples were two–three times longer than those of helium free controls. The minimum creep rate of implanted specimens decreased to about 40% of that of control samples, mirroring the changes in the creep lifetimes. Elongation at creep rupture was slightly decreased by helium implantation.

(2) Although most of the fracture surfaces of helium injected specimens showed a ductile fracture mode, regions which contained intergranular decohesion were observed. Besides induction of intercrystalline separation, the tendency of necking in ductile fracture surfaces was reduced by helium.

Acknowledgements

This study was financially supported by the Budget for Nuclear Research of the Ministry of Education, Culture, Sports, Science and Technology, based on the screening and counseling by the Atomic Energy Commission.

References

[1] T. Muroga, T. Nagasaka, K. Abe, V.M. Chernov, H. Matsui, D.L. Smith, et al., J. Nucl. Mater. 307–311 (2002) 547.
[2] T. Muroga, T. Nagasaka, in: Fusion Energy 2000, 18th Conference Proceeding, Sorrento, October 2000, FTP1/09.
[3] R.J. Kurtz, K. Abe, V.M. Chernov, V.A. Kazakov, G.E. Lucas, H. Matsui, et al., J. Nucl. Mater. 283–287 (2000) 70.
[4] R.J. Kurtz, M.L. Hamilton, J. Nucl. Mater. 283–287 (2000) 628.
[5] K. Fukumoto, T. Yamamoto, N. Nakao, S. Takahashi, H. Matsui, J. Nucl. Mater. 307–311 (2002) 610.
[6] K. Natesan, W.K. Soppet, A. Purohit, J. Nucl. Mater. 307–311 (2002) 585.
[7] K. Matsumoto, T. Kataoka, J. Nucl. Mater. 67 (1977) 97.
[8] N. Yamamoto, J. Nagakawa, H. Shiraishi, H. Kamitsubo, I. Kohno, T. Shikata, J. Nucl. Sci. Technol. 28 (1991) 1001.
[9] N. Yamamoto, J. Nagakawa, K. Shiba, Key Eng. Mater. 171–174 (2000) 115.